

[文章编号] 1671-587X(2024)04-0939-08

DOI:10.13481/j.1671-587X.20240407

PTMC/PVP温控收缩性纳米纤维膜与小鼠成纤维细胞的生物相容性及其对大鼠皮肤全层缺损的修复作用

刘丽萍¹, 李驰宇², 杨 韬¹, 王少如¹, 刘 昀¹, 刘国民², 程志强³, 罗云纲⁴, 刘志辉¹

(1. 吉林大学口腔医院修复科, 吉林 长春 130021; 2. 吉林大学第二医院骨科, 吉林 长春 130041;

3. 吉林农业大学资源与环境学院, 吉林 长春 130118; 4. 吉林大学第一医院

净月分院口腔医学中心, 吉林 长春 130118)

[摘要] **目的:** 探讨温控收缩性聚三亚甲基碳酸酯 (PTMC) /聚乙烯吡咯烷酮 (PVP) 纳米纤维膜对小鼠成纤维细胞生物学行为的影响及对大鼠全层皮肤缺损的修复作用, 并阐明其可能的作用机制。**方法:** 体外实验选用小鼠成纤维L929细胞, 分为对照组和实验组 (采用PTMC/PVP纳米纤维膜处理), CCK-8法检测2组细胞增殖活性, 活/死细胞染色实验观察2组细胞中活/死细胞数量, 细胞骨架染色实验观察2组细胞形态表现。体内实验选用12只6周龄雄性SD大鼠, 随机分为对照组和实验组, 每组6只, 建立全层皮肤缺损模型, 实验组大鼠采用PTMC/PVP纳米纤维膜治疗, 术后拍照观察, 第0、3、6和12天时计算2组大鼠创面愈合率, 术后第6和12天切取2组大鼠皮肤创面和周围组织, 采用HE染色观察皮肤创面和周围组织病理形态表现, Masson三色染色观察2组大鼠皮肤创面组织中胶原蛋白沉积情况, CD31免疫组织化学染色检测2组大鼠皮肤创面组织中血管形成数量。**结果:** CCK-8实验, 实验组细胞增殖活性在第1、3和5天均呈升高趋势, 与对照组比较差异无统计学意义 ($P>0.05$)。活/死细胞染色实验, 与对照组比较, 实验组细胞密度和数量无明显变化且以活细胞为主。细胞骨架染色实验, 实验组和对照组细胞均呈梭形且细胞伸展。体内实验, 第3、6和12天时, 与对照组比较, 实验组大鼠创面愈合率升高 ($P<0.01$), 12 d时实验组大鼠创面愈合率为95.45%, 创面基本愈合。HE染色, 与对照组比较, 第12天实验组大鼠创面皮肤结构更接近正常皮肤, 有丰富的肉芽组织、规则的表皮结构和新血管生成。Masson三色染色, 与对照组比较, 实验组大鼠创面组织中胶原蛋白沉积量更多。免疫组织化学染色, 与对照组比较, 实验组大鼠创面组织中CD31表达增多, 表明血管形成数量增加。**结论:** PTMC/PVP温控收缩性纳米纤维膜具有良好的生物相容性, 且能促进大鼠皮肤全层缺损的修复, 其作用机制可能与增强基底细胞增殖活性有关。

[关键词] 伤口敷料; 机械力学; 温控收缩性; 聚三亚甲基碳酸酯/聚乙烯吡咯烷酮; 纳米纤维; 静电纺丝

[中图分类号] R318.08 **[文献标志码]** A

[收稿日期] 2023-07-22

[基金项目] 吉林省科技厅科技发展计划项目 (20220204124YY)

[作者简介] 刘丽萍 (1997—), 女, 山东省潍坊市人, 在读硕士研究生, 主要从事纳米纤维临床应用方面的研究。

[通信作者] 刘志辉, 教授, 博士研究生导师 (E-mail: liu_zh@jlu.edu.cn);

罗云纲, 教授, 博士研究生导师 (E-mail: luoygju@sina.com)

Biocompatibility of PTMC/PVP temperature-controlled shrinkage nanofiber membrane with mouse fibroblasts and its repairment effect on full-thickness skin defects in rats

LIU Liping¹, LI Chiyu², YANG Tao¹, WANG Shaoru¹, LIU Yun¹, LIU Guomin², CHENG Zhiqiang³, LUO Yungang⁴, LIU Zhihui¹

(1. Department of Prosthodontics, Stomatology Hospital, Jilin University, Changchun 130021, China;

2. Department of Orthopedics, Second Hospital, Jilin University, Changchun 130041, China;

3. School of Resources and Environment, Jilin Agricultural University, Changchun 130118, China;

4. Stomatology Center, Jingyue Campus, First Hospital, Jilin University, Changchun 130118, China)

ABSTRACT Objective: To discuss the effect of temperature-controlled shrinkage poly(trimethylene carbonate) (PTMC)/poly(vinylpyrrolidone) (PVP) nanofiber membrane on the biological behavior of mouse fibroblasts and the repairment effect on full-thickness skin defects in the rats, and to clarify the potential mechanism. **Methods:** The murine L929 fibroblast cells were used in the *in vitro* experiments and were divided into control group and experimental group (treated with PTMC/PVP nanofiber membranes). The proliferation activities of the cells in two groups were detected by CCK-8 assay; the numbers of live/dead cells in two groups were observed by live/dead cell staining; the morphology of the cells was observed by cytoskeletal staining. A total of 12 six-week-old male SD rats were selected in the *in vivo* experiment, and were randomly divided into control group and experimental group, and there were six rats in each group. The full-thickness skin defect model was established, and the rats in experimental group were treated with PTMC/PVP nanofiber membranes. The photographs were taken after operation, and the wound healing rates of the cells in two groups were calculated on the 0, 3rd, 6th, and 12th days. On the 6th and 12th days after operation, the skin samples around the wound of the rats in two groups were taken, and the histopathology of the wound skin and adjacent tissue was detected by HE staining; the collagen deposition in wound skin tissue of the rats in two groups was observed by Masson trichrome staining; the numbers of angiogenesis in wound skin tissue of the rats were detected by CD31 immunohistochemical staining. **Results:** The CCK-8 assay results showed that the proliferation activity of the cells in experimental group showed an increasing trend on the 1st, 3rd, and 5th days, and there was no significant difference in the proliferation activities of the cells between experimental group and control group ($P > 0.05$). The live/dead cell staining experiment results showed that compared with control group, the cell density and number of the cells in experimental group had no significant changes, and were predominantly live cells. The cytoskeletal staining results showed that the cells in experimental and control groups appeared spindle-shaped and well-spread. In the *in vivo* experiments, on the 3rd, 6th, and 12th days, compared with control group, the wound healing rates of the cells in experimental group were increased ($P < 0.01$), and the wound healing rate of the cells was 95.45% on the 12th day, indicating nearly complete healing of the wound. The HE staining showed that on the 12th day, the wound skin structure of the cells in experimental group was more similar to the normal skin, and there was abundant granulation tissue, regular epidermal structure, and new blood vessel formation. The Masson trichrome staining results showed that compared with control group, the collagen deposition in wound tissue of the rats in experimental group was increased. The immunohistochemical staining results showed that the expression of CD31 in wound tissue of the rats in experimental group was increased, indicating the increasing of the number of angiogenesis. **Conclusion:** The PTMC/PVP thermoresponsive nanofiber membranes exhibit

good biocompatibility and can promote the repairment of full-thickness skin defects in the rats; its mechanism may be related to the enhancement of proliferation activity of the basal cells.

KEYWORDS Wound dressing; Mechanical mechanics; Temperature-controlled shrinkage; Polytrimethylene carbonate /polyvinylpyrrolidone; Nanofiber; Electrospinning

皮肤是人体最大的器官, 是身体抵御外界因素入侵的第一道屏障^[1]。口腔颌面部的皮肤位于人体突出且暴露的位置, 极易受到创伤而导致软组织缺损^[2]。在伤口愈合过程中, 慢性或面积较大的伤口很难通过自我收缩闭合, 缝合是促进伤口闭合的金标准技术^[3], 但其具有留下疤痕或感染的风险, 传统敷料如纱布和绷带等具有不同程度的吸收性, 在去除后会导致损伤和组织生长不全^[4]。目前伤口敷料的研究主要着重于材料的生化功能, 如在敷料中添加生物活性物质, 从而赋予敷料抗菌^[5-6]、血管形成^[7]和抗炎^[8]等功能, 但均存在价格昂贵、制备复杂和不良反应较大等弊端。近年来, 胚胎伤口独特的无创愈合方式逐渐引起生物医学领域的关注。研究^[9]表明: 在胚胎伤口的愈合过程中围绕胚胎伤口边缘的细胞前缘形成肌动蛋白束, 肌动蛋白束收缩并施加力可将伤口边缘拉在一起, 最终实现伤口的完美愈合。受到胚胎伤口无创快速愈合方式的启发, 利用材料的机械收缩性能缩小伤口的面积、促进伤口的闭合和愈合已经成为制备伤口敷料的新的研究方向之一^[10-12]。

聚乙烯吡咯烷酮 (polyvinylpyrrolidone, PVP) 是一种水溶性高分子化合物, 具有良好的生物相容性、吸湿性和粘性, 被广泛应用于生物医疗领域^[13-14]。聚三亚甲基碳酸酯 (polytrimethylene carbonate, PTMC) 是一种可生物降解的非晶体聚合物, 具有良好的生物相容性和力学性能^[15]。在本课题组前期研究^[16]中, 通过静电纺丝技术成功制备了具有温控收缩性的PTMC/PVP纳米纤维膜, 对其理化性质表征和体外温控收缩性能进行了研究, 结果表明: PTMC/PVP纳米纤维具有周期性分布的多孔纺锤状结构, 并且当PTMC与PVP的比例为1:3时具有最强的收缩性, 其收缩率随温度的升高而增大, 同时能在30 min内将大鼠离体皮肤的创伤面积缩小至70%左右。在此基础上, 本研究通过体外细胞实验和体内实验对PTMC/PVP (1:3) 纳米纤维膜进行深入研究, 探讨其细胞相容性及对大鼠皮肤全层缺损的修复作用, 为其进一步临床应用提供依据。

1 材料与方法

1.1 细胞、实验动物、主要试剂和仪器

小鼠成纤维L929细胞购自中国科学院上海细胞库。12只6周龄雄性SD大鼠购自吉林大学实验动物中心, 动物使用许可证号: SYXK202306061, 体质量180~200 g。PTMC (相对分子质量为378 000) 购自济南岱罡生物工程有限公司, PVP (相对分子质量为630 000) 购自上海阿拉丁生化科技股份有限公司, 二氯甲烷 (dichloromethane, DCM) 和N, N-二甲基甲酰胺 (N, N-dimethylformamide, DMF) 购自上海麦克林生化科技股份有限公司, 青霉素-链霉素溶液、磷酸盐缓冲液 (phosphate buffer solution, PBS)、DMEM高糖培养基和胰蛋白酶购自美国Hyclone公司, 胎牛血清 (fetal bovine serum, FBS) 购自美国BI公司, CCK-8试剂盒购自美国Invitrogen公司, 活/死细胞染色试剂盒购自上海贝博生物科技有限公司, DAPI染液和TRITC-Phalloidin染液购自北京索莱宝科技有限公司, 脱毛膏购自中国利洁时家化有限公司, 4%多聚甲醛购自中国白鲨生物科技有限公司。静电纺丝机购自北京艾博智业有限公司, 多功能酶标仪、恒温细胞培养箱、离心机和旋转石蜡切片机购自美国ThermoFisher公司, 倒置荧光显微镜和正置光学显微镜购自日本Olympus公司, 石蜡包埋机购自湖北泰微医疗科技有限公司, 自动脱水机和自动染色机购自德国Leica公司。

1.2 PTMC/PVP纳米纤维膜的制备

根据本课题组前期研究^[16]的方法制备PTMC/PVP纳米纤维膜。将PTMC和PVP (1:3, W/W) 溶解在DCM和DMF (3:1, W/W) 混合物中, 室温搅拌6 h后制得静电纺丝前体溶液 (3%), 将其进行静电纺丝5 h制得纳米纤维膜, 其中电纺参数为电压15 kV, 流速2 mL·h⁻¹, 针头距离接收器的距离20 cm, 针头内径21 G。将所有制备好的膜置于真空干燥箱中24 h。

1.3 PTMC/PVP纳米纤维膜的细胞相容性检测

1.3.1 细胞培养 将L929细胞接种于含10%FBS和1%青霉素-链霉素溶液的DMEM高糖培养基中, 置于37℃、5% CO₂恒温细胞培养箱中培养,

当细胞生长密度达80%时使用胰蛋白酶消化传代,用于后续实验。

1.3.2 CCK-8法检测各组细胞增殖活性 将PTMC/PVP纳米纤维膜经紫外照射杀菌后置于96孔细胞培养板底部,以每孔 1.5×10^3 个细胞的密度将L929细胞接种于96孔细胞培养板中,每2d更换1次培养基,设不含PTMC/PVP纳米纤维膜的L929细胞为对照组。第1、3和5天更换为含有10% CCK-8溶液的培养基,置于恒温细胞培养箱中避光孵育2h,采用酶标仪检测各组细胞培养上清液在450 nm波长处的吸光度(A)值,以A值代表细胞增殖活性。

1.3.3 活/死细胞染色实验检测各组活/死细胞数量 将PTMC/PVP纳米纤维膜紫外照射杀菌并置于24孔细胞培养板底部,以每孔 1×10^4 个细胞的密度将L929细胞接种于24孔细胞培养板中。培养48h后弃去培养基,加入根据说明书配制好的Calcein-AM/PI染色工作液,置于细胞培养箱中避光孵育15min后,弃去工作液并用PBS缓冲液冲洗2次。采用荧光倒置显微镜观察细胞染色情况和数量,活细胞发出绿色荧光,而死细胞发出红色荧光。设不含PTMC/PVP纳米纤维膜的L929细胞为对照组。

1.3.4 细胞骨架染色实验检测各组细胞形态表现 细胞分组和处理方法见“1.3.3”。细胞培养48h后弃去培养基,PBS缓冲液冲洗2次后用4%多聚甲醛固定细胞15min,再用0.2% Triton X-100透化处理15min,PBS缓冲液冲洗2次。加入根据说明书配制好的TRITC-Phalloidin染色工作液室温避光孵育30min,PBS缓冲液冲洗2次,再加入DAPI染液避光孵育30s后,弃去工作液并用PBS缓冲液冲洗2次。采用荧光倒置显微镜观察细胞形态表现,细胞骨架发出红色荧光,细胞核发出蓝色荧光。

1.4 大鼠全层皮肤缺损模型的构建和实验分组

12只雄性SD大鼠禁食禁水后采用戊巴比妥钠($40 \text{ mg} \cdot \text{kg}^{-1}$)腹腔注射麻醉,剃除并用脱毛膏去除大鼠背部毛发后,75%乙醇进行皮肤消毒,用打孔器在大鼠的背部制备直径为10mm的圆形全层皮肤缺损。12只SD雄性大鼠随机分为对照组(创面用生理盐水处理)和实验组(创面用直径20mm的圆形PTMC/PVP纳米纤维膜覆盖),对2组大鼠进行相应处理后,均使用无菌纱布覆盖创

面。在0、3、6和12d时拍照记录,采用Image J软件测量并计算创面面积,采用创面愈合率评估创面愈合情况。创面愈合率=(初始创面面积-第n天创面面积/初始创面面积 $\times 100\%$ 。

1.5 组织学染色观察2组大鼠皮肤创面组织病理形态表现、胶原蛋白沉积情况和血管形成数量

术后第6和12天,取大鼠皮肤创面及周围组织,用4%多聚甲醛固定,包埋在石蜡中并制成厚度为 $4 \mu\text{m}$ 的组织切片,采用HE染色、Masson三色染色和CD31免疫组织化学染色后用显微镜采集图像,分别观察大鼠皮肤创面组织病理形态表现、胶原蛋白沉积情况和CD31表达情况,CD31阳性表达增加则表示血管形成数量增多。

1.6 统计学分析

采用SPSS 25.0统计软件进行统计学分析。2组细胞增殖活性和大鼠皮肤创面愈合率均呈正态分布,以 $\bar{x} \pm s$ 表示,多组间样本均数比较采用单因素方差分析,组间样本均数两两比较采用LSD-*t*检验,2组间样本均数比较采用两独立样本*t*检验。以 $P < 0.05$ 为差异有统计学意义。

2 结果

2.1 PTMC/PVP纳米纤维膜的细胞相容性

采用CCK-8法检测PTMC/PVP纳米纤维膜使用后各组L929细胞的增殖活性。第1、3和5天L929细胞增殖活性呈升高趋势,与对照组比较,实验组细胞增殖活性差异无统计学意义($P > 0.05$)。见图1。

采用活/死细胞染色实验观察2组L929细胞的生存能力。与对照组比较,实验组细胞密度和数量

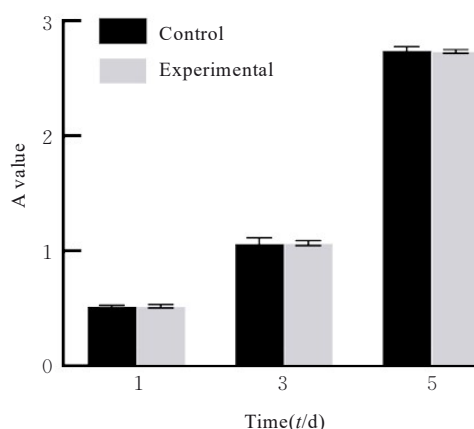
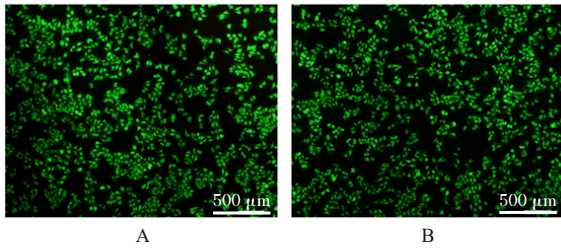


图1 CCK-8法检测不同时间2组细胞增殖活性

Fig.1 Proliferation activities of cells in two groups at different time points detected by CCK-8 method

无明显变化, 且均以活细胞 (绿色荧光) 为主, 仅有少量死细胞 (红色荧光)。见图 2。

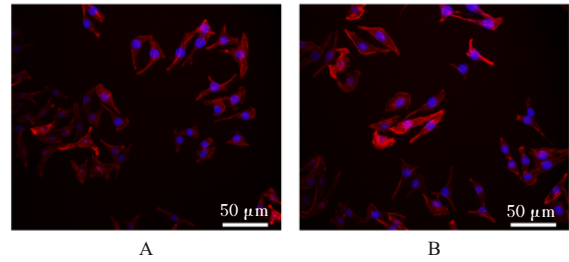
采用细胞骨架染色实验观察 2 组 L929 细胞形态表现。对照组和实验组 L929 细胞均呈梭形且细胞伸展。见图 3。



A: Control group; B: Experimental group.

图 2 培养 2 d 时 2 组细胞活/死细胞染色情况

Fig. 2 Live/dead cell staining of cells in two groups after cultured for 2 d



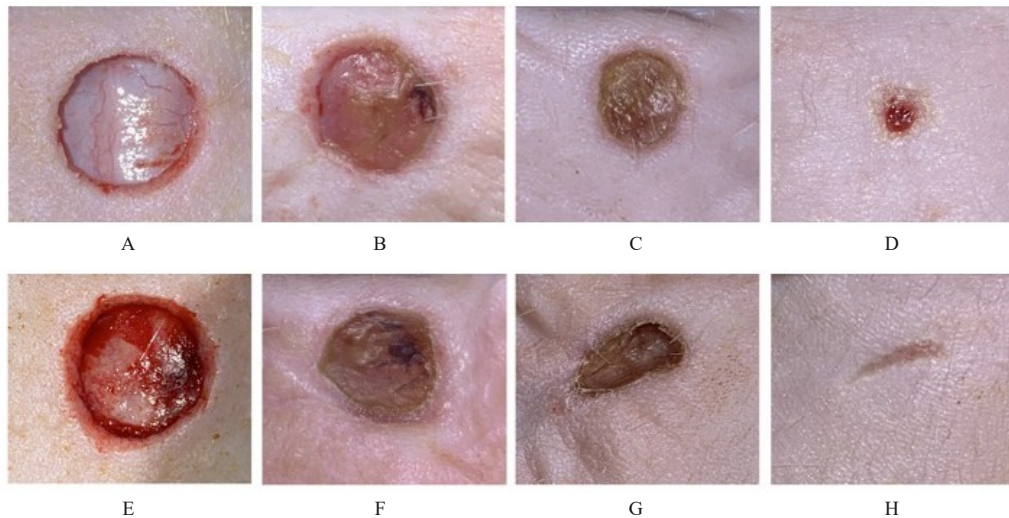
A: Control group; B: Experimental group.

图 3 培养 2 d 时 2 组细胞骨架染色情况

Fig. 3 Cytoskeleton staining of cells in two groups after cultured for 2 d

2.2 2 组大鼠皮肤创面愈合率

术后第 12 天时可见实验组大鼠皮肤创面面积较小, 基本愈合, 而对照组大鼠皮肤创面仍有少量结痂。见图 4。



A—D: Control group; E—H: Experimental group; A, E: 0 d; B, F: 3 d; C, G: 6 d; D, H: 12 d.

图 4 术后不同时间点 2 组大鼠皮肤创面愈合情况

Fig. 4 Skin wound healing of rats in two groups at different time points after surgery

术后第 3、6 和 12 天时, 实验组大鼠皮肤创面愈合率均高于对照组 ($P < 0.01$)。见图 5。

2.3 2 组大鼠皮肤创面组织病理形态表现、胶原蛋白沉积情况和血管形成情况

HE 染色: 治疗 12 d 后, 2 组大鼠皮肤创面均进行了一定程度的再上皮化, 与对照组比较, 实验组大鼠皮肤创面具有更成熟的上皮组织、丰富的毛囊和新生血管 (图 6A~6D)。Masson 染色: 与对照组比较, 实验组大鼠皮肤创面组织有更密集和排列更好的胶原蛋白 (蓝色) 沉积 (图 6E~6H)。CD31 免疫组织化学染色: 与对照组比较, 实验组

大鼠皮肤创面组织中 CD31 表达 (棕黄色区域) 增多, 表明血管形成数量增加 (图 6I~6L)。

3 讨论

近年来, 受胚胎伤口无创愈合方式的启发, 材料的机械收缩性已经成为促进皮肤伤口闭合的研究热点之一。BLACKLOW 等^[17] 制备了热响应收缩性聚 N-异丙基丙烯酰胺 (poly N-isopropylacrylamide, PNIPAm) 活性黏合剂敷料, 利用该敷料的机械活性和黏性能够有效加速伤口闭合和伤口愈合。THEOCHARIDIS 等^[18] 制备了一

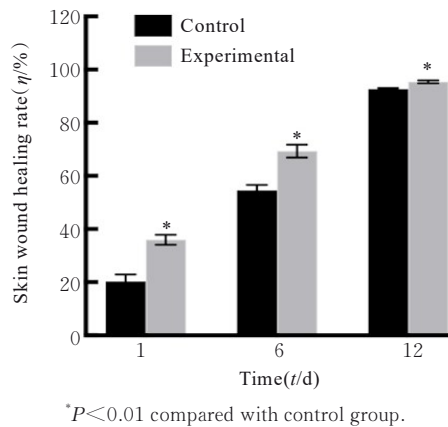


图5 术后不同时间点2组大鼠皮肤创面愈合率

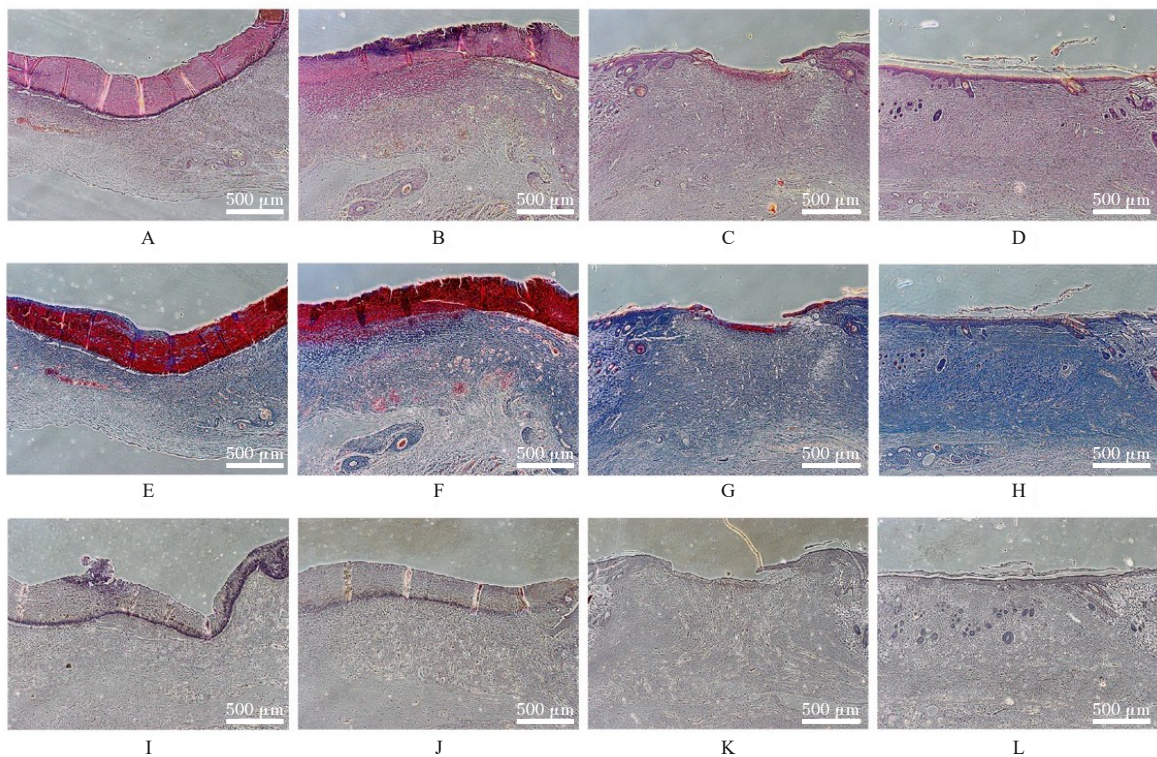
Fig. 5 Skin wound healing rates of rats in two groups at different time points after surgery

种应变程序化贴片, 基于材料的形状记忆机制, 机械收缩糖尿病患者伤口, 促进糖尿病患者伤口闭合和再上皮化。

本课题组前期研究^[16]制备出用于促进伤口闭合的温控收缩性PTMC/PVP纳米纤维膜, 并且已经对其理化性质表征和体外温控收缩性进行了研

究, 结果表明: 利用PTMC的温控收缩性和出色的力学性能及PVP的亲水性和黏附性, PTMC/PVP纳米纤维膜能够有效缩小大鼠离体皮肤缺损模型的面积, 加速伤口闭合。在前期研究的基础上, 本研究进一步探讨了PTMC/PVP纳米纤维膜的生物相容性以及大鼠全层皮肤缺损模型的修复作用。

细胞相容性是设计生物材料植入物和医疗设备的首要条件, 细胞增殖活性是评估伤口敷料生物特性的重要指标。本研究中CCK-8实验、活/死细胞染色实验和细胞骨架染色实验结果显示: PTMC/PVP纳米纤维膜对L929细胞无毒性作用, 且对L929细胞形态也无明显影响, 表明PTMC/PVP纳米纤维膜具有良好的细胞相容性。PTMC和PVP均是美国食品药品监督管理局(Food and Drug Administration, FDA)批准的具有良好生物相容性的聚合物材料。PTMC具有独特的降解性能, 包括抵抗非酶降解和表面降解机制, 使PTMC在降解过程中能够保持结构稳定性, 同时其降解产物呈中性, 避免了酸性降解产物对细胞及伤口产生的



A—D: HE staining; E—H: Masson trichrome staining; I—L: CD31 immunohistochemical staining; A, C, E, G, I, K: Control group; B, D, F, H, J, L: Experimental group; A, B, E, F, I, J: 6 d; C, D, G, H, K, L: 12 d.

图6 术后不同时间点2组大鼠皮肤创面组织病理形态表现、胶原蛋白沉积情况和血管形成情况

Fig. 6 Pathomorphology, collagen deposition, and angiogenesis of skin wound tissue of rats in two groups at different time points after surgery

炎症刺激^[15]。而PVP作为亲水性聚合物,已经在制药、生物医学和营养保健领域中广泛用作载体^[19]。

本研究进一步通过体内实验验证PTMC/PVP纳米纤维膜对大鼠全层皮肤缺损的修复作用,第3、6和12天时实验组大鼠伤口愈合率明显高于对照组,表明通过该纳米纤维膜的机械牵拉作用能够有效缩小伤口的面积,促进伤口的愈合,与相关研究结果^[11]一致。本研究中HE染色结果表明:PTMC/PVP纳米纤维膜能够有效促进皮肤伤口处的再上皮化。沉积和重塑适当的胶原蛋白对于伤口愈合至关重要,本研究中Masson三色染色结果表明:PTMC/PVP纳米纤维膜能够促进大鼠皮肤创面胶原蛋白的沉积。血管化通过向伤口部位提供氧气和营养物质并清除代谢废物,在伤口修复中起着至关重要的作用,为了研究PTMC/PVP纳米纤维膜促进大鼠皮肤创面愈合的效果,本研究评估了血管生成的程度。CD31是一种跨膜蛋白,在早期血管生成中表达,在促进伤口愈合方面发挥着至关重要的作用^[20-21]。本研究中CD31免疫组织化学染色结果表明:PTMC/PVP纳米纤维膜可以促进皮肤组织修复过程中的血管生成。快速的伤口收缩能够促进伤口的修复过程^[22],可能是由于伤口的收缩过程增强了基底细胞的增殖活性,减少了伤口的炎症反应,从而促进了伤口的愈合。研究^[23]表明:抑制Yes关联蛋白(Yes-associated protein, YAP)和丝裂原活化蛋白激酶(mitogen-activated protein kinase, MAPK)能够阻断创面的收缩反应,因此YAP和MAPK/细胞外调节蛋白激酶(extracellular regulatory protein kinase, ERK)信号通路的调节也可能影响伤口的愈合进程。

综上所述,温控收缩性PTMC/PVP纳米纤维膜具有良好的细胞相容性,并能够通过机械收缩性缩小大鼠全层皮肤缺损处的面积,促进皮肤缺损处的胶原蛋白沉积、血管生成和再上皮化,加速皮肤缺损的修复过程。PTMC/PVP纳米纤维膜在促进伤口闭合和伤口愈合方面具有良好的应用前景。

利益冲突声明:

所有作者声明不存在利益冲突。

作者贡献声明:

刘丽萍参与研究设计和论文撰写,李弛宇和杨韬参与数据收集和分析,王少如和刘昀参与论文结果分析和讨论,刘国民和程志强参与研究设计和实验指导,罗云纲和刘志辉参与论文撰写指导和论文审校。

[参考文献]

- [1] ESKILSON O, ZATTARIN E, BERGLUND L, et al. Nanocellulose composite wound dressings for real-time pH wound monitoring [J]. *Mater Today Bio*, 2023, 19: 100574.
- [2] GRAÇA M F P, MELO-DIOGO D D, CORREIA I J, et al. Electrospun asymmetric membranes as promising wound dressings: a review [J]. *Pharmaceutics*, 2021, 13(2): 183.
- [3] ANANDA B B, VIKRAM J, RAMESH B S, et al. A comparative study between conventional skin sutures, staples adhesive skin glue for surgical skin closure [J]. *Int Surg J*, 2019, 6(3): 775.
- [4] BRUMBERG V, ASTRELINA T, MALIVANOVA T, et al. Modern wound dressings: hydrogel dressings [J]. *Biomedicines*, 2021, 9(9): 1235.
- [5] WANG X, ZHAO D H, LI Y T, et al. Collagen hydrogel with multiple antimicrobial mechanisms as antibacterial wound dressing [J]. *Int J Biol Macromol*, 2023, 232: 123413.
- [6] LIAO W D, YANG D, XU Z L, et al. Antibacterial collagen-based nanocomposite dressings for promoting infected wound healing [J]. *Adv Healthc Mater*, 2023, 12(15): e2203054.
- [7] ZEHRA M, ZUBAIRI W, HASAN A, et al. Oxygen generating polymeric nano fibers that stimulate angiogenesis and show efficient wound healing in a diabetic wound model [J]. *Int J Nanomedicine*, 2020, 15: 3511-3522.
- [8] HUANG C, DONG L L, ZHAO B H, et al. Anti-inflammatory hydrogel dressings and skin wound healing [J]. *Clin Transl Med*, 2022, 12(11): e1094.
- [9] MARTIN P, LEWIS J. Actin cables and epidermal movement in embryonic wound healing [J]. *Nature*, 1992, 360(6400): 179-183.
- [10] LI M, LIANG Y P, HE J H, et al. Two-pronged strategy of biomechanically active and biochemically multifunctional hydrogel wound dressing to accelerate wound closure and wound healing [J]. *Chem Mater*, 2020, 32(23): 9937-9953.
- [11] HU J Y, WEI T, ZHAO H, et al. Mechanically active adhesive and immune regulative dressings for wound closure [J]. *Matter*, 2021, 4(9): 2985-3000.
- [12] DONG R, GUO B. Smart wound dressings for wound healing [J]. *Nano Today*, 2021, 41: 101290.
- [13] PANT B, PARK M, PARK S J. Drug delivery applications of core-sheath nanofibers prepared by coaxial

- electrospinning: a review[J]. *Pharmaceutics*, 2019, 11(7): 305.
- [14] 徐 密, 张 良, 何志仙. 纳米罗勒精油/聚乙烯吡咯烷酮-聚乙烯醇水凝胶伤口敷料制备及性能表征[J]. *复合材料学报*, 2024, 41(2): 748-760.
- [15] FUKUSHIMA K. Poly(trimethylene carbonate)-based polymers engineered for biodegradable functional biomaterials[J]. *Biomater Sci*, 2016, 4(1): 9-24.
- [16] LIU L P, LI T, SUN M L, et al. Preparation of temperature-controlled shrinkage PTMC/PVP core-shell nanofibrous membrane with spindle-knotted structure for accelerating wound closure[J]. *Mater Lett*, 2022, 324: 132601.
- [17] BLACKLOW S O, LI J, FREEDMAN B R, et al. Bioinspired mechanically active adhesive dressings to accelerate wound closure[J]. *Sci Adv*, 2019, 5(7): eaaw3963.
- [18] THEOCHARIDIS G, YUK H, ROH H, et al. A strain-programmed patch for the healing of diabetic wounds[J]. *Nat Biomed Eng*, 2022, 6(10): 1118-1133.
- [19] FRANCO P, DE MARCO I. The use of poly(N-vinyl pyrrolidone) in the delivery of drugs: a review [J]. *Polymers (Basel)*, 2020, 12(5): 1114.
- [20] YE J J, LI L F, HAO R N, et al. Phase-change composite filled natural nanotubes in hydrogel promote wound healing under photothermally triggered drug release[J]. *Bioact Mater*, 2023, 21: 284-298.
- [21] ZHAO X, LIANG Y P, HUANG Y, et al. Physical double-network hydrogel adhesives with rapid shape adaptability, fast self-healing, antioxidant and NIR/pH stimulus-responsiveness for multidrug-resistant bacterial infection and removable wound dressing[J]. *Adv Funct Materials*, 2020, 30(17): 1910748.
- [22] ZHAO Y D, YI B C, HU J L, et al. Double cross-linked biomimetic hyaluronic acid-based hydrogels with thermo-stimulated self-contraction and tissue adhesiveness for accelerating post-wound closure and wound healing[J]. *Adv Funct Materials*, 2023, 33(26): 2300710.
- [23] LI Z, HUANG J J, JIANG Y G, et al. Novel temperature-sensitive hydrogel promotes wound healing through YAP and MEK-mediated mechanosensitivity[J]. *Adv Healthc Mater*, 2022, 11(23): e2201878.